Inelastic electron scattering from ^{9}Be

R. W. Lourie, W. Bertozzi, T. N. Buti, J. M. Finn, F. W. Hersman,*
C. Hyde, J. Kelly,† M. A. Kovash, and S. Kowalski
Department of Physics and Laboratory for Nuclear Science, Massachusetts Institute of Technology, Cambridge, Massachusetts 02139

M. V. Hynes
Los Alamos National Laboratory, University of California, Los Alamos, New Mexico 87545

B. E. Norum
Department of Physics, University of Virginia, Charlottesville, Virginia 22901

B. L. Berman
Lawrence Livermore National Laboratory, University of California, Livermore, California 94550
(Received 29 December 1982)

The electromagnetic form factors have been measured for the lowest two $T=\frac{3}{2}$ states in ^{9}Be at 14.393 and 16.976 MeV, the positive-parity state at 17.490 MeV, and a level of previously unknown J^π at 16.671 MeV. The range of effective momentum transfer is $0.9 \leq q_e \leq 2.5$ fm^{-1}. The data for the $T=\frac{3}{2}$ states show considerable deviation from the results of intermediate-coupling shell-model calculations. In particular, for $q_e \leq 1.5$ fm^{-1}, where the $M1$ multipole dominates, the data lie well above these calculated values. There is some evidence that the state at 16.671 MeV has positive parity. The results of single-particle shell-model and Nilsson-model calculations are compared with the data for this state. The experimental form factor for the 17.490-MeV state can be fitted with single-particle shell-model results in the $2s$-$1d$ space.

[NUCLEAR REACTIONS ^{9}Be(e,e'), sharp states from 14 to 18 MeV; measured form factors at 160°, 140°, $0.9 \leq q_e \leq 2.5$ fm^{-1}; comparison with shell-model and Nilsson-model calculations.]

I. INTRODUCTION

We have undertaken an extensive program of electron and proton scattering from ^{9}Be. As part of this program, we have studied several narrow levels in ^{9}Be by inelastic electron scattering. These results are reported in this paper. In particular, we have measured the electromagnetic form factors for the two $T=\frac{3}{2}$ states at 14.393 MeV ($J^\pi=\frac{3}{2}^-$) and 16.976 MeV ($J^\pi=\frac{1}{2}^-$), for a positive-parity level at 17.490 MeV, and for a state of unknown J^π at 16.671 MeV, for effective momentum transfers q_e between 0.9 and 2.2 fm^{-1}. The electroexcitation of these states was first reported by Clerc *et al.*,[1] at low momentum transfers. Later experiments by Bergstrom *et al.*[2] extended these results to $q=1.1$ fm^{-1}. All four of these states share the characteristic that their form factors are essentially completely transverse.

Narrow $T=\frac{3}{2}$ odd-parity levels in ^{9}Be near 15 MeV excitation have been predicted by several authors,[3-5] based upon shell-model calculations within the $1p$ shell. The results of Cohen and Kurath[4] will be compared with the data here.

The positive-parity level at 17.490 MeV cannot be treated successfully by any calculation that is restricted to configurations entirely within the $1p$ shell. The $2s$-$1d$ and $1g$ shells would produce positive-parity levels, with the energetics of the transition favoring the $2s$-$1d$ shell. Accordingly, single-particle shell-model calculations were done in an attempt to classify this state. At best such an approach can only identify the dominant shell-model configuration.

Although not conclusive, this work provides some evidence that the 16.671-MeV state has positive parity. Assuming this parity assignment, form factors are calculated for $1p$ to $2s$-$1d$ transitions for comparison with the data. Since ^{9}Be is known to be a deformed nucleus [it exhibits a ground-state rotational band ($J^\pi=\frac{3}{2}^-,\frac{5}{2}^-,\frac{7}{2}^-$) and a large quadrupole moment], Nilsson-model calculations also are compared with the data here.

II. EXPERIMENT AND DATA ANALYSIS

A. Introduction

Electron scattering has three great advantages for nuclear-structure studies. First, since the interaction with the nucleus is electromagnetic, the reaction mechanism is well understood. Second, because of the weakness of the interaction, the probe does not appreciably disturb the target structure and allows the use of perturbation theory with respect to the nuclear system for the calculation of cross sections; in most cases, first-order perturbation theory is adequate. Finally, electron scattering allows the variation of the three-momentum q transferred to the target while the excitation energy ω is kept fixed (in contrast to real photon processes which require $q=\omega$). This enables one to measure the momentum-transfer dependence of the transition matrix elements.

The definitions and symbols used in this paper are the

same as in the recent paper on ^{18}O (Ref. 6). Further details on the formalism of electron scattering can be found in Refs. 7–9.

B. Experimental details

The data for this experiment were obtained at the MIT Bates Linear Accelerator Laboratory. The accelerator[10] and the spectrometer together with its detection system[11,12] have been discussed in detail elsewhere.

Most of the data were taken at a scattering angle of 160°, although some points at 90° and 140° were measured as well. Electron energies ranged between 100 and 285 MeV, producing effective momentum transfers q_e from 0.9 to 2.5 fm^{-1}. The targets used for these measurements were of pure beryllium metal having thicknesses between 15 and 30 mg/cm^2. Cross sections were measured for most states in ^9Be up to 18 MeV excitation. This work concentrates on the four narrow states between 14 and 18 MeV.

Several features contribute to the high performance of the Bates electron-scattering facility. First is the energy-loss mode of operation which allows use of a large fraction of the accelerated beam and hence the measurement of small cross sections without any sacrifice of resolution. Second is the focal-plane detection system, which when coupled with the computer software, produces the high-resolution spectra observed at Bates. The detection system consists of a vertical drift chamber (VDC), two transverse multiwire proportional counters, and two Čerenkov counters. The VDC measures the track position along the momentum direction and the angle in the bend plane with respect to the central ray entering the spectrometer. The transverse arrays measure the track position transverse to the momentum direction. The transverse position is related linearly (in first order) to the horizontal (scattering) angle by the optical transformation of the spectrometer. The coincidence of the Čerenkov detectors provides the fiducial start signal for all timing measurements.

The computer software accomplishes two tasks. The first is a series of tests to determine whether the signals from the focal-plane detectors correspond to a true electron event. Once an event passes these tests, the three parameters (the momentum position and the horizontal and vertical angles) are computed. Knowledge of these coordinates allows the planar-detector measurements to be projected back to the actual (curved) focal surface. This eliminates the broadening of a peak introduced by the use of planar detectors. The kinematic broadening of the peaks which results from the finite acceptance of the spectrometer is corrected for as well, by use of the horizontal angle measurement. The overall resolution obtained with this system is typically $\Delta P/P \simeq 2\times 10^{-4}$.

A representative spectrum observed in this experiment is shown in Fig. 1. The FWHM of 43 keV for the narrow 14.393-MeV state corresponds to an energy resolution $\Delta E/E$ of 2.4×10^{-4}.

C. Data analysis

The method of data analysis has been described in Ref. 6. Further details can be found in Refs. 13 and 14.

The scattered-electron spectra first are corrected for dead-time effects and detector efficiencies. Then the peak areas (and hence cross sections) are obtained by means of a line shape fitting program. In this program, the shape of each peak is treated as the convolution of the optical resolution function of the system with the shape that would result if the system had infinitely fine resolution (this latter shape accounts for the combined effects of radiation losses, ionization losses, etc.). Convoluting the radiative effects with the optical resolution function is more accurate than merely applying multiplicative correction factors (see Ref. 15). A peak with a natural width of at least the order of the resolution width is treated as the triple convolution of the optical resolution function, the radiation tail, and the natural line shape of the peak (for which a Breit-Wigner shape was used).

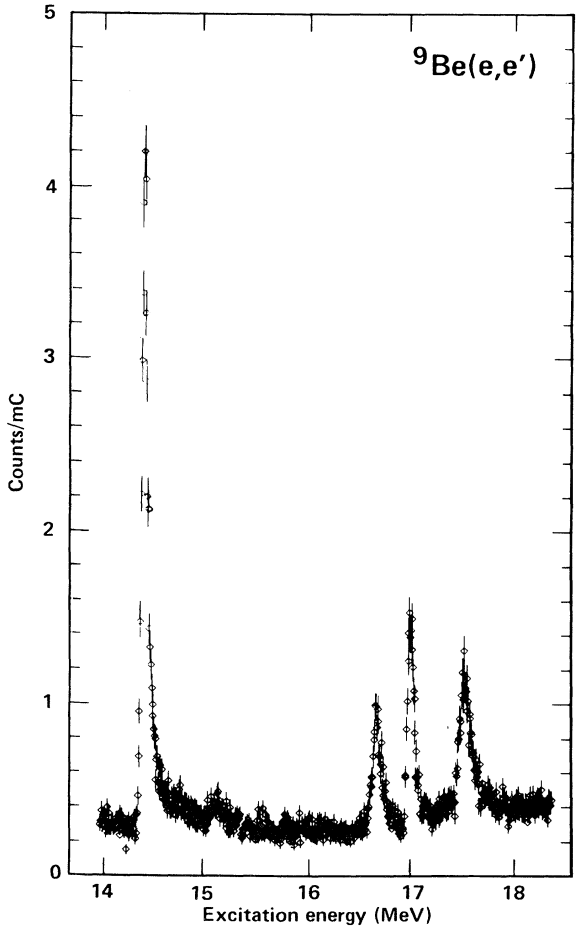

FIG. 1. Representative spectrum for inelastic electron scattering from ^9Be (present work), showing the four sharp states at 14.4, 16.7, 17.0, and 17.5 MeV.

The function used to describe the system resolution is a Gaussian, modified to include an asymmetry parameter. The radiation-tail function, which accounts for the processes of ionization and bremsstrahlung and for the Schwinger corrections, is described in detail in Refs. 14 and 15.

The fitting procedure consists of assigning estimated values to the peak parameters for all peaks in the fitting region and including a background of linear, quadratic, or cubic form. The parameters are then varied to obtain a

maximum-likelihood fit. The code is based upon the routine CURFIT (from Ref. 16), but modified[17] to account correctly for Poisson statistics. The un-normalized cross section for a given state now is obtained from the area under the fitted peak and from the values of the experimental solid angle, the effective target thickness, and the electron beam flux.

D. Normalization

Under the same experimental conditions both BeO and pure Be targets were exposed. The ^{16}O absolute cross section is well known, and a phase-shift code using the best-fit ^{16}O charge distribution was used to calculate the ^{16}O elastic cross section (see Ref. 18). The ^{9}Be elastic peak occurring in the BeO spectrum is normalized to the ^{16}O elastic peak via these computed values. The ^{9}Be elastic peak observed using the pure Be target is then normalized to the one observed using the BeO target, and the inelastic cross sections observed using the Be target were in turn normalized to the elastic cross section.

The ^{9}Be elastic-scattering results are in very good agreement with the results from other laboratories,[19,20] as is shown in Fig. 2. In fact, in the range of momentum transfer spanned, the present data are of far better statistical precision.

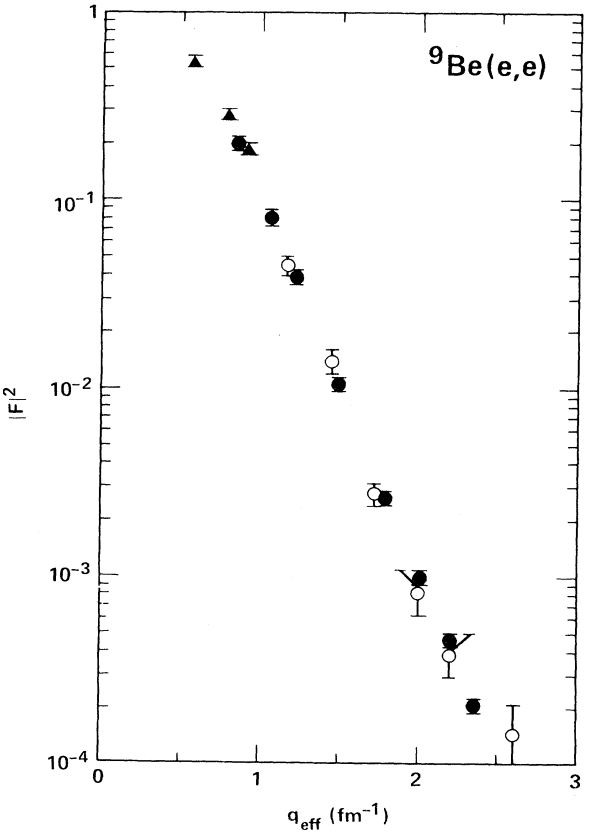

FIG. 2. Elastic electron-scattering form factor for ^{9}Be, showing the agreement between the present results and those from other laboratories: solid circles, present work; open circles, Ref. 19; triangles, Ref. 20.

E. Uncertainties

There are two primary sources of experimental uncertainty: the statistical uncertainties associated with the counting statistics and the fitting procedure, and the systematic uncertainties associated with the various system parameters, mainly the central energy of the beam and the scattering angle. Beam energy calibration is accomplished by measuring, in the scattered-electron spectrum, the recoil-energy differences of several nuclei (^{18,17,16}O, ^{9}Be) and their excited states. The final electron momentum (energy) is determined by the VDC channel in which the electron is detected and by the VDC and spectrometer system constants. The energy scale could be calibrated by this procedure to $\Delta E_0/E_0 \sim 5$ to 10×10^{-4}. When there was not a sufficient number of peaks in a spectrum to use this method accurately, the energy was taken to be that defined by the switchyard via its energy slits; this is accurate to $\sim 0.1\%$. The resulting uncertainty in the final form factors does not exceed 5%. Scattering-angle uncertainties, associated with the positioning of the spectrometer ($\sim 0.02°$) and the angle between the beam and the normal to the target (~ 5 mrad), are less than 1%.

Finally, the (systematic) uncertainty introduced by the normalization procedure is typically 1 to 2 % and is never larger than $\sim 8\%$ (at the minimum in the ^{16}O form factor at $q \simeq 1.6$ fm^{-1}).

III. RESULTS AND DISCUSSION

A. Experimental results

The measured form factors for the states at 14.393, 16.671, 16.976, and 17.490 MeV are tabulated in Tables I through IV. The measurements of Refs. 1 and 2 show that the longitudinal part of these form factors is very small. For those data points from this work where a Rosenbluth separation of the transverse and longitudinal components was possible it was found that the form factors were completely transverse to within their statistical error bars. The separation was made at $q = 1.46$ and 1.70 fm^{-1} and for scattering angles of 90° and 160°. Consequently, the quantity listed in the tables is the square of

TABLE I. Transverse form factor ($\theta = 160°$) for the 14.393-MeV state in ^{9}Be ($J^\pi = \frac{3}{2}^-$, $T = \frac{3}{2}$).

E_0 (MeV)	q_e (fm^{-1})	$\lvert F_T \rvert^2 \times 10^4$	Uncertainty (%)
99.95	0.940	1.58	2.0
105.18	0.989	1.77	2.1
115.12	1.087	2.05	2.1
124.61	1.184	2.14	2.5
130.92	1.233	2.30	2.0
139.77	1.330	2.20	2.0
154.92	1.475	2.14	2.3
169.76	1.620	1.89	2.9
180.17	1.716	1.77	2.2
204.76	1.955	1.16	2.3
229.51	2.194	0.676	3.0
249.07[a]	2.271	0.473	4.4
270.15[a]	2.462	0.218	8.5

[a] $\theta = 140°$.

the transverse form factor

$$|F_T|^2=\frac{\eta\sigma_{\text{meas}}}{Z^2\sigma_{\text{Mott}}}\frac{1}{(\frac{1}{2}+\tan^2\theta/2)},$$

where the recoil factor

$$\eta=1+\frac{2E_0}{M_T}\sin^2\frac{\theta}{2},$$

σ_{meas} and σ_{Mott} are the measured and Mott cross sections, Z and M_T are the charge and mass of the target nucleus, E_0 is the incident electron energy, and θ is the scattering angle.

The agreement between the present data and those of Ref. 2, where the two data sets overlap, is good: The present results are a bit lower for the states at 14.4 and 17.0 MeV, a bit higher for the state at 16.7 MeV, and nearly the same for the one at 17.5 MeV (see below).

B. The $T=\frac{3}{2}$ states

The isospin T of the levels at 14.393 and 16.976 MeV has been determined to be $\frac{3}{2}$ by stripping reactions. The 14.393-MeV state was investigated by Lynch *et al.*[21] using the ^{7}Li(^{3}He,p)^{9}Be reaction, whereas the reactions ^{7}Li(d,p)^{8}Li and ^{7}Li(d,γ)^{9}Be were used by Woods and Wilkinson[22] to identify the isospin of the 16.976-MeV state. These first two $T=\frac{3}{2}$ states in ^{9}Be are the analogs of the ground and first excited states of ^{9}Li.

Cohen and Kurath[4] have done extensive intermediate-coupling calculations in the 1p shell. They determine effective two-body interactions by fitting energy-level data for various states in nuclei throughout the 1p shell. The calculations assume that only 1p shell configurations contribute to all of these states. They use 17 parameters (15 matrix elements and 2 single-particle energies) with general two-body matrix elements and consider nuclei with $A=6$ to $A=16$. This will be referred to here as the CK calculation. Once the interaction is determined, wave functions and energy levels are calculated. They predict four $T=\frac{3}{2}$ levels above 13 MeV in ^{9}Be, two of which are seen in electron scattering and are known to have $T=\frac{3}{2}$. In order to compare the results of their calculation with the results of this work, form factors were calculated. These calculations were performed using the transition-density matrix formalism, which allows the reduced matrix element of any one-body operator to be written in terms of a transition-density matrix and the reduced matrix elements of the operator between single-particle states.[23] The computer code MICRODENSITY (Ref. 23) was used to calculate the form factors from the transition-density matrices for proton and neutron configurations. Kurath[24] has supplied these, as derived from the CK wave functions. They are listed in Table V. The possible multipoles that can contribute to the excitation of the $\frac{3}{2}^-$ 14.393-MeV state are $M1$, $M3$, and $E2$, while only the $M1$ and $E2$ multipoles can contribute to the $\frac{1}{2}^-$ 16.976-MeV state. The q dependence of the cross sections at low momentum transfer is of $M1$ character.[1] The oscillator parameter ($b_0=1.67$ fm) for the harmonic-oscillator wave functions was taken from the elastic magnetic-scattering results of Rand *et al.*[25]

Figures 3 and 4 show the experimental form factors and the CK predictions. The calculated $M1$ and $M3$ form factors provide a reasonable description of the data for the 14.393-MeV state for momentum transfers greater than 1.5 fm^{-1}. The lower-q data stand above the calculated curve by about 35%.

This may be due to underestimating the $M1$ strength although the calculation will also underestimate the low q strength because of the fact that the $E2$ convection current contribution vanishes when the initial and final states have the same radial wave function.[23] Since the CK wave functions are restricted to the 1p shell and expanded in a spherical harmonic oscillator basis, then in this case no convection current contribution is possible. Flanz *et al.*[26] report a similar result when the CK wave functions are used to describe the transverse form factor of the 4.43 MeV state in ^{12}C. Indeed, connecting the convective transverse current to a phenomenological longitudinal

TABLE II. Transverse form factor ($\theta=160°$) for the 16.671-MeV state in ^{9}Be.

E_0 (MeV)	q_e (fm^{-1})	$\lvert F_T\rvert^2\times10^5$	Uncertainty (%)
99.95	0.929	5.28	2.2
115.12	1.075	2.49	9.2
124.61	1.173	1.27	21.5
154.92	1.464	1.34	18.7
169.76	1.609	4.31	9.0
180.17	1.705	6.17	5.7
204.76	1.944	6.37	6.4
229.51	2.183	4.72	5.8

TABLE III. Transverse form factor ($\theta=160°$) for the 16.976-MeV state in ^{9}Be ($J^\pi=\frac{1}{2}^-$, $T=\frac{3}{2}$).

E_0 (MeV)	q_e (fm^{-1})	$\lvert F_T\rvert^2\times10^5$	Uncertainty (%)
99.95	0.929	7.02	2.0
115.12	1.074	8.61	2.3
124.61	1.171	9.16	3.2
130.92	1.220	9.09	2.5
139.77	1.317	8.99	2.7
154.92	1.462	7.83	2.7
169.76	1.607	6.80	2.8
180.17	1.703	6.12	2.1
204.76	1.943	3.93	4.3
229.51	2.181	1.87	7.2

TABLE IV. Transverse form factor ($\theta=160°$) for the 17.490-MeV state in ^{9}Be ($J^\pi\leq\frac{7}{2}^+$).

E_0 (MeV)	q_e (fm^{-1})	$\lvert F_T\rvert^2\times10^4$	Uncertainty (%)
99.95	0.925	1.34	2.0
115.12	1.071	1.23	3.2
124.61	1.169	1.01	5.8
130.92	1.217	0.914	8.7
139.77	1.314	0.806	5.7
154.92	1.460	0.828	6.3
169.76	1.605	0.814	8.2
180.17	1.701	0.830	5.9
204.76	1.940	0.873	10.6
229.51	2.179	0.431	5.8

TABLE V. $1p$-shell transition-density matrix elements to the lowest two $T=\frac{3}{2}$ states in ^{9}Be. (The listed quantity is for proton configurations; the neutron density is the negative of the proton density.)

		$1p_{3/2}\rightarrow 1p_{3/2}$			$1p_{3/2}\rightarrow 1p_{1/2}$		$1p_{1/2}\rightarrow 1p_{3/2}$		$1p_{1/2}\rightarrow 1p_{1/2}$	
$\lambda^a=$	3	2	1	0	2	1	2	1	1	0
$(\frac{3}{2}^-,\frac{3}{2})$	0.2364	−0.4291	0.2120	−0.0244	0.0744	0.2054	−0.0098	0.0873	0.0644	0.0345
$(\frac{1}{2}^-,\frac{3}{2})$		−0.0794	−0.1823		0.1952	−0.1945	−0.0132	−0.0212	−0.0143	

[a] λ is the transition multipolarity.

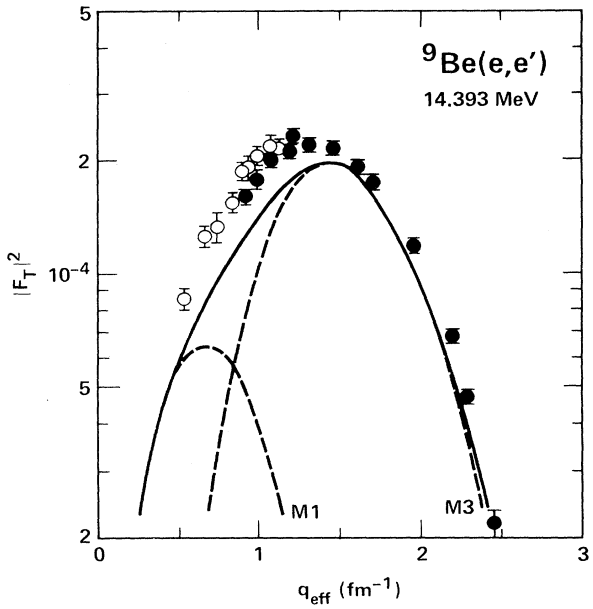

FIG. 3. Transverse form factor for the $J^\pi=\frac{3}{2}^-$, $T=\frac{3}{2}$ state in ^{9}Be at 14.393 MeV, showing the inadequacy of an intermediate-coupling-model prediction: solid circles, present work; open circles, Ref. 2. The solid curve is the sum of the dashed curves, which represent the $M1$ and $M3$ form factors computed from the CK wave functions (Ref. 4).

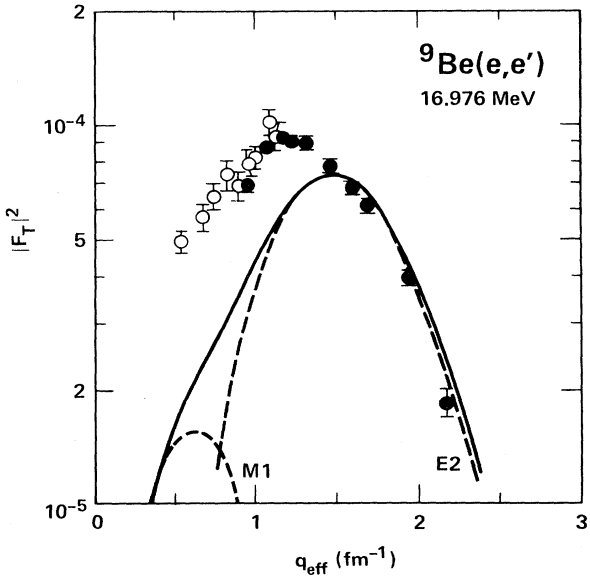

FIG. 4. Transverse form factor for the $J^\pi=\frac{1}{2}^-$, $T=\frac{3}{2}$ state in ^{9}Be at 16.976 MeV, showing the inadequacy of an intermediate-coupling-model prediction: solid circles, present work; open circles, Ref. 2. The solid curve is the sum of the dashed curves, which represent the $M1$ and $E2$ form factors computed from the CK wave functions (Ref. 4).

charge density via the continuity equation[27] successfully accounts for the low q strength in the transverse form factor for the 4.43 MeV state in ^{12}C, as does a large-basis shell-model calculation[28] since p-f and s-d shell configurations allow convective currents. However, using the method of Ref. 27 to introduce a sufficient convection contribution to remedy this discrepancy for these states in ^{9}Be would introduce unacceptably large longitudinal components. Also, even if the $M1$ form factor were scaled up there would still be disagreement with the data at intermediate q which cannot be removed in the case of the 16.976-MeV state. In addition, the CK wave functions predict a larger longitudinal ($C2$) contribution for both these states than is observed. The relatively high excitation energy of the $T=\frac{3}{2}$ states in conjunction with their narrow widths implies a complex structure—in particular, that configurations outside the $1p$ shell may be quite important for the description of these states.

C. The 16.671-MeV state

Two prominent features of the 16.671-MeV state are (a) its sharp diffraction minimum at $q\sim 1.2$ fm^{-1} and (b) its second maximum, which has the same magnitude as the first. Although J^{π} for this state has not been determined unambiguously, the measurements of Ref. 1 indicate that the q dependence of the cross section is of $M2$ or spin-flip $E1$ character, which in turn implies positive parity. Further evidence for this parity assignment is the observation of this state in the photoneutron data of Hughes *et al.*,[29] where $E1$ transitions from the negative-parity ground state would be favored. Assuming positive parity therefore, possible spherical shell-model and Nilsson-model form factors have been calculated. Candidate shell-model states are in the $2s$-$1d$ shell. The form factor for an $M2$ transition of the unpaired $1p_{3/2}$ neutron to the $1d_{5/2}$ or to the $2s_{1/2}$ shell has been given in Ref. 7. Bergstrom *et al.*[2] found that only these two $M2$ transitions provided a reasonable description of their data; the $1p_{3/2}\rightarrow 1d_{3/2}$ $M2$ form factor peaks at too high a momentum transfer and the form factors for the $E1$ transitions, while of the right shape, fall well below the data. The $M2$ $1p_{3/2}\rightarrow 1d_{5/2}$ and $1p_{3/2}\rightarrow 2s_{1/2}$ form factors are compared with the data in Fig. 5(a). The oscillator parameter b_0 for the $2s_{1/2}$ transition is 1.65 fm and is 1.89 fm for the $1d_{5/2}$ transition. Additionally, a neutron effective charge $e_n=1.0$ was used in the $1d_{5/2}$ calculation. The values of all these parameters were taken from Ref. 2. It was found in the present work that no other values would improve the fit to the second maximum without degrading considerably the fit to the first. Although both calculations fit the first maximum equally well, the $1p_{3/2}\rightarrow 1d_{5/2}$ transition provides a better description of the second maximum. Even so, it underestimates the data by 16% at the peak and by 50% at the highest-q point. The neutron effective charge required is also quite large (1.0). If this state has any $E1$ part, such a large effective charge could introduce longitudinal components into the form factor if the charge were to represent orbital currents (equivalent to configurations that are missing owing to the truncation of the model space). If the charge represents spin polarization, i.e., a renormalization of the magnetic moment, then there is no problem with longitudinal components.

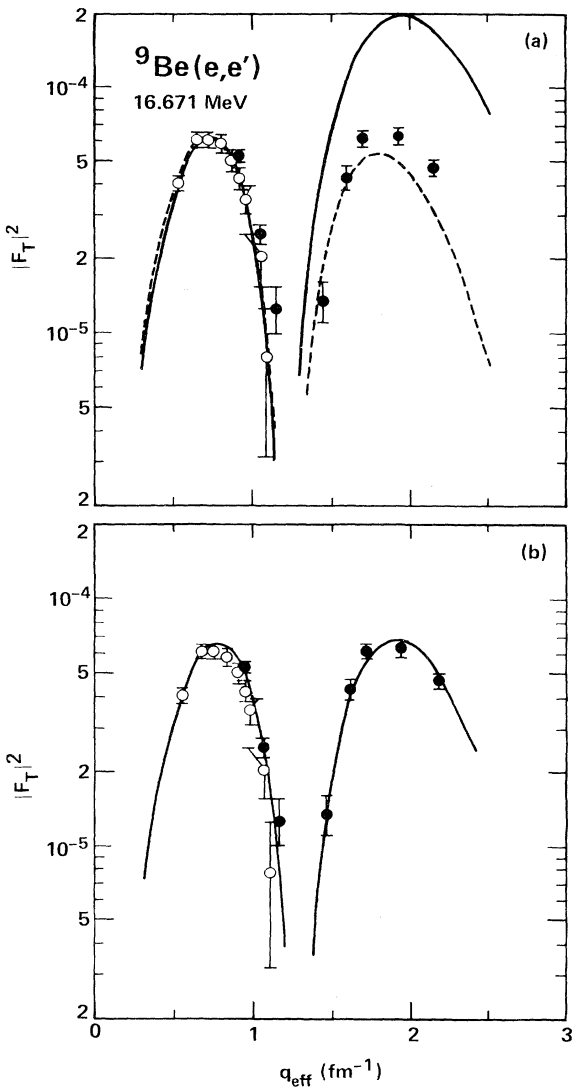

FIG. 5. Transverse form factor for the state in ^{9}Be at 16.671 MeV, compared with theoretical predictions: solid circles, present work; open circles, Ref. 2. (a) shows the $M2$ form factors computed from the (spherical) shell model: solid line, $1p_{3/2}\rightarrow 2s_{1/2}$; dashed line, $1p_{3/2}\rightarrow 1d_{5/2}$. (b) shows the $M2$ form factor computed from the (deformed) Nilsson model either for spin $\frac{1}{2}$ with neutron effective charge $e_n=0.6$ or for spin $\frac{5}{2}$ with $e_n=1.8$.

Since ^{9}Be is known to be a deformed nucleus, the pure single-particle spherical shell model would not be expected to provide a realistic description in any case. Consequently, Nilsson-model calculations were performed. In this model, ^{9}Be is described as an odd neutron strongly coupled to a deformed rigid ^{8}Be core; the ground state is the $\frac{3}{2}^{-}[101]$ orbital; and the transition corresponds to the promotion of the valence neutron to the orbitals which reduce to the $2s$-$1d$ shell for zero deformation. The reduced matrix element for such a transition is

$$\langle J'K'||\hat{T}_\lambda(q)||JK\rangle=[(2J+1)(2J'+1)]^{1/2}\sum_{jj'}C_{j'K'}C_{jK}\langle j'||\hat{T}_\lambda(q)||j\rangle \times\left[(-1)^{J'-j'}\begin{pmatrix}J' & \lambda & J\\ -K' & \mu & K\end{pmatrix}\begin{pmatrix}j' & \lambda & j\\ -K' & \mu & K\end{pmatrix}+\begin{pmatrix}J' & \lambda & J\\ K' & \mu & K\end{pmatrix}\begin{pmatrix}j' & \lambda & j\\ K' & \mu & K\end{pmatrix}\right],$$

where the $C_{jK'}$ ($C_{j'K'}$) are the coefficients of expansion of the initial (final) Nilsson model state in the spherical basis. These coefficients have been tabulated by Davidson[30] for various values of the deformation parameter β. With the assumption of an inert core $\langle j'||T_\lambda||j\rangle$ is simply a single-particle reduced matrix element.

Slight *et al.*[20] have shown that the observed energy spacings between the Nilsson basis states and the value of the intrinsic quadrupole moment determine the deformation parameter β and the spin-orbit parameter k unambiguously. They found $\beta=0.3$ and $k=0.069$. Bergstrom *et al.*[2] obtained satisfactory fits to the first maximum of the data with $\frac{3}{2}^-[101]\rightarrow\frac{1}{2}^+[220]$ $M2$ transitions and for a $\frac{3}{2}^-[101]\rightarrow\frac{1}{2}^+[211]$ $E1$ transition; but the fits in Ref. 2 all underestimate the second maximum, by a factor of 8 for the $E1$ and by factors of 4 and 2 for the $M2$ spin-$\frac{5}{2}$ and spin-$\frac{1}{2}$ states, respectively.

Since all these transitions have the same functional form, a computer fit of that form to all of the data was performed. When the result of this fit is compared to a theoretical expression it may be interpreted as determining an overall scale factor N, the neutron effective charge e_n, and the oscillator parameter b_0. The values of these parameters extracted from the theoretical expressions are most reasonable for the $\frac{3}{2}^-[101]\rightarrow\frac{1}{2}^+[220]$ (spin-$\frac{1}{2}$) $M2$ transition, which gives $b_0=1.8$ fm, $e_n=0.6$, and $N=1.4$. An identical fit to the data is obtained for the $\frac{3}{2}^-[101]\rightarrow\frac{1}{2}^+[220]$ (spin-$\frac{5}{2}$) $M2$ transition, with $b_0=1.8$ fm, $e_n=1.8$, and $N=1.3$. The results of this calculation are displayed in Fig. 5(b). The agreement is quite good, the most serious discrepancy being the point at $q_e=1.7$ fm^{-1}, which is 25% above the (scaled) calculation. However, the Nilsson model predicts this state to be at only 5 MeV in excitation energy. The fact that all the various calculations tried yield good qualitative and fair quantitative agreement with the data would, along with the results of Refs. 1 and 29, support a positive-parity assignment for this state.

D. The 17.490-MeV state

The form factor for this state is essentially flat between 1 and 2 fm^{-1} and then drops by a factor of 2 between 2 and 2.2 fm^{-1}. This indicates that many multipoles are contributing to this transition. The rapid falloff occurs on the high-q side of the highest contributing multipole. If this multipole could be identified, the range of possible spin assignments would be limited. If this state could be described as predominantly due to the promotion of the valence neutron to either the $1d_{5/2}$ or $1d_{3/2}$ shells, then the high-q behavior would be $M4$ or $E3$ for a $1p_{3/2}\rightarrow1d_{5/2}$ transition and $E3$ for a $1p_{3/2}\rightarrow1d_{3/2}$ transition. Figure 6(a) shows the $M2$ (scaled down by 2.2) and the $M4$ (scaled down by 6.7) components of the $1p_{3/2}\rightarrow1d_{5/2}$ transition. The $M4$ is indistinguishable from the $E3$ scaled up by 4. This combination of multipoles produces a reasonable description of the data except in the intermediate-q range. The case of a $1p_{3/2}\rightarrow1d_{3/2}$ neutron transition involving $E1$ and $E3$ multipoles is shown in Fig. 6(b). Oscillator parameters of 1.67 and 1.78 fm were used for the $1d_{5/2}$ and $1d_{3/2}$ cases, respectively. It is seen that the high-q behavior of the data is not as well described by this $E3$ multipole as it is by the $M4$ in Fig. 6(a).

IV. CONCLUSIONS AND SUMMARY

The intermediate-coupling wave functions of Cohen and Kurath,[4] which provide the standard description of low-lying spectra and moments of $1p$-shell nuclei, have been shown to exhibit serious deficiencies when used to predict form factors for the two $T=\frac{3}{2}$ states. In particular, their

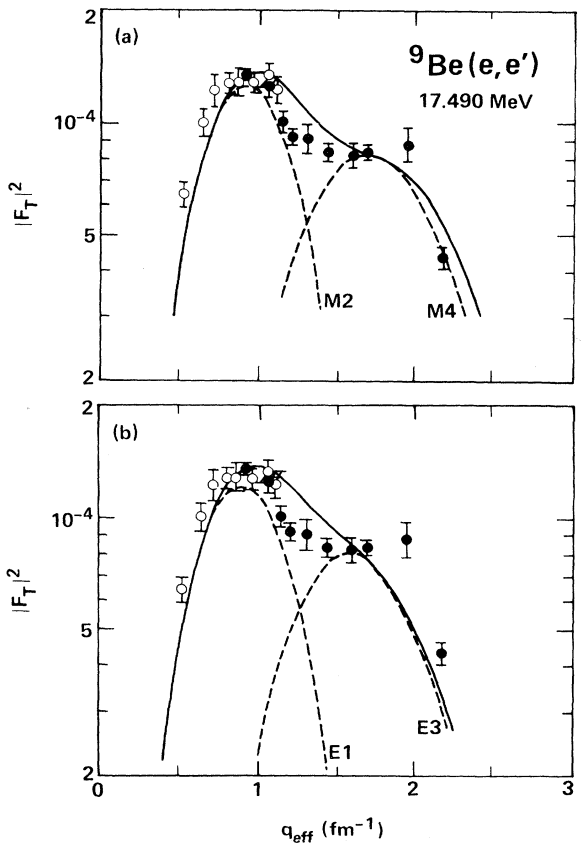

FIG. 6. Transverse form factor for the positive-parity state in ^{9}Be at 17.490 MeV, compared with arbitrarily scaled shell-model predictions: solid circles, present work; open circles, Ref. 2. (a) shows the best fit using $M2$ and $M4$ multipoles for a $1p_{3/2}\rightarrow1d_{5/2}$ transition and (b) shows the best fit using $E1$ and $E3$ multipoles for a $1p_{3/2}\rightarrow1d_{3/2}$ transition; for both cases the (best-fit) solid line is the sum of the individual multipole form factors (dashed lines).

results underestimate the low-q strength in both these states. The fact that no convection current contribution can be generated in a model space restricted to the (harmonic oscillator) $1p$ shell is most likely responsible for the lack of low-q strength in these calculations. Enlarging the shell-model basis beyond the $1p$ shell appears to be important to describe these data.

The general shape of the form factor of the 16.671-MeV state can be reproduced by either spherical shell-model or Nilsson-model calculations, but one must consider the size of the neutron effective charges, their physical interpretation in terms of currents and spin polarization, and their effect upon the longitudinal part of the form factor. Moreover, it was impossible to uniquely identify the configuration of this state in either the shell or Nilsson models. An unambiguous determination of the contributing multipole or multipoles was also not possible since the theoretical expressions for the form factors of the various transitions considered here had the same analytic form. For a given transition it was possible to determine an overall scale factor, the oscillator parameter, and the neutron effective charge. Perhaps the best description of this state is provided by the $\frac{3}{2}^-[101]\rightarrow\frac{1}{2}^+[220]$ (spin-$\frac{1}{2}$) Nilsson calculation, which requires an effective charge of only 0.6. The apparent absence of any $E3$ or $M4$ form factors suggests that they are forbidden by angular momentum selection rules which in turn supports a spin assignment of $J=\frac{1}{2}$.

The 17.490 state's form factor drops off rapidly beyond 1.9 fm^{-1} indicating that the highest contributing multipole is being observed in this region of momentum transfer. Comparison with shell-model results in the $1d$ shell indicates that a $1p_{3/2}\rightarrow 1d_{5/2}$ neutron transition provides a reasonable description of the data below 1 fm^{-1} and above 1.5 fm^{-1} while a $1d_{3/2}$ description only agrees with the low momentum transfer data.

Note added in proof. Recent analysis of lower energy 90° data on the 14.393-MeV state indicates the presence of some longitudinal component. Its contribution to the data presented, however, is $<2\%$.

ACKNOWLEDGMENTS

We are indebted to B. Murdock and B. Pugh for several very valuable discussions and assistance and to D. Kurath for providing us with the density matrix elements. One of us (R.W.L.) wishes to acknowledge the support of the Fannie and John Hertz Foundation. The work was supported by the U. S. Department of Energy under Contract No. DE-AC02-76ER03069.

*Present address: Physics Department, University of New Hampshire, Durham, NH 03824.

†Present address: Los Alamos National Laboratory, Los Alamos, NM 87545.

[1]H. G. Clerc, K. J. Wetzel, and E. Spamer, Phys. Lett. 20, 667 (1966).

[2]J. C. Bergstrom, I. P. Auer, M. Ahmad, F. J. Kline, J. H. Hough, H. S. Caplan, and J. L. Groh, Phys. Rev. C 7, 2228 (1973).

[3]D. Amit and A. Katz, Nucl. Phys. 58, 338 (1964).

[4]S. Cohen and D. Kurath, Nucl. Phys. 73, 1 (1965).

[5]F. C. Barker, Nucl. Phys. 83, 418 (1966).

[6]B. E. Norum, M. V. Hynes, H. Miska, W. Bertozzi, J. Kelly, S. Kowalski, F. N. Rad, C. P. Sargent, T. Sasanuma, W. Turchinetz, and B. L. Berman, Phys. Rev. C 25, 1778 (1982).

[7]T. de Forest and J. D. Walecka, Adv. Phys. 15, 1 (1966).

[8]J. M. Eisenberg and W. Greiner, *Excitation Mechanisms of the Nucleus* (North-Holland, Amsterdam, 1970).

[9]H. Überall, *Electron Scattering from Complex Nuclei* (Academic, New York, 1971).

[10]W. Bertozzi, J. Haimson, C. P. Sargent, and W. Turchinetz, IEEE Trans. Nucl. Sci. 14, 191 (1967).

[11]W. Bertozzi, M. V. Hynes, C. P. Sargent, C. Creswell, P. C. Dunn, A. Hirsch, M. Leitch, B. Norum, F. N. Rad, and T. Sasanuma, Nucl. Instrum. Methods 141, 457 (1977).

[12]W. Bertozzi, M. V. Hynes, C. P. Sargent, W. Turchinetz, and C. Williamson, Nucl. Instrum. Methods 162, 211 (1979).

[13]B. E. Norum, Ph.D. thesis, MIT, 1979 (unpublished).

[14]M. V. Hynes, Ph.D. thesis, MIT, 1978 (unpublished).

[15]J. C. Bergstrom, in Proceedings of the MIT 1967 Summer Study (unpublished), p. 251.

[16]P. R. Bevington, *Data Reduction and Error Analysis for the Physical Sciences* (McGraw-Hill, New York, 1969).

[17]M. V. Hynes, B. E. Norum, and B. Peterson (unpublished).

[18]H. Miska, B. Norum, M. V. Hynes, W. Bertozzi, S. Kowalski, F. N. Rad, C. P. Sargent, T. Sasanuma, and B. L. Berman, Phys. Lett. 83B, 165 (1979).

[19]M. Bernheim, T. Stovall, and D. Vinciguerra, Nucl. Phys. A97, 488 (1967).

[20]A. G. Slight, T. E. Drake, and G. R. Bishop, Nucl. Phys. A208, 157 (1973).

[21]B. Lynch, G. M. Griffiths, and T. Lauritsen, Nucl. Phys. 65, 641 (1965).

[22]J. B. Woods and D. H. Wilkinson, Nucl. Phys. 61, 661 (1965).

[23]H. C. Lee, Atomic Energy of Canada Limited Report No. AECL-4839, 1974.

[24]D. Kurath, private communication.

[25]R. E. Rand, R. Frosch, and M. R. Yearian, Phys. Rev. 144, 859 (1966).

[26]J. B. Flanz, R. S. Hicks, R. A. Lindgren, G. A. Peterson, A. Hotta, B. Parker, and R. C. York, Phys. Rev. Lett. 41, 1642 (1978).

[27]D. Cha, Phys. Rev. C 21, 1672 (1980).

[28]K. Amos and I. Morrison, Phys. Rev. C 19, 2108 (1979).

[29]R. J. Hughes, R. H. Sambell, E. G. Muirhead, and B. M. Spicer, Nucl. Phys. A238, 189 (1975).

[30]J. P. Davidson, *Collective Models of the Nucleus* (Academic, New York, 1968).